

Article

Techno-Economic Analysis of Large Scale Production of Poly(oxymethylene) Dimethyl Ether Fuels from Methanol in Water-Tolerant Processes

Yannic Tönges¹, Vincent Dieterich², Sebastian Fendt², Hartmut Spliethoff² and Jakob Burger^{1,*}

¹ Laboratory of Chemical Process Engineering, Campus Straubing for Biotechnology and Sustainability, Technical University of Munich, Uferstraße 53, 94315 Straubing, Germany

² TUM School of Engineering and Design, Technical University of Munich, Boltzmannstraße 15, 85748 Garching, Germany

* Correspondence: burger@tum.de

Abstract: Poly(oxymethylene) dimethyl ether (OME) are a much-discussed and promising synthetic and renewable fuel for reducing soot and, if produced as e-fuel, CO₂ emissions. OME production is generally based on the platform chemical methanol as an intermediate. Thus, the OME production cost is strongly dependent on the methanol cost. This work investigates OME production from methanol. Seven routes for providing methanolic formaldehyde solutions are conceptually designed for the first time and simulated in a process simulator. They are coupled with a state-of-the-art OME synthesis to evaluate the economics of the overall production chain from methanol to OME. For a plant size of 100 kt/a, the average levelized product cost of OME is 79.08 EUR/t plus 1.31 times the cost of methanol in EUR/t.

Keywords: methanolic formaldehyde solution; poly(oxymethylene) dimethyl ether (OME); techno-economic analysis



Citation: Tönges, Y.; Dieterich, V.; Fendt, S.; Spliethoff, H.; Burger, J. Techno-Economic Analysis of Large Scale Production of Poly(oxymethylene) Dimethyl Ether Fuels from Methanol in Water-Tolerant Processes. *Fuels* **2023**, *4*, 1–18. <https://doi.org/10.3390/fuels4010001>

Academic Editors: Nicolaus Dahmen, Olaf Toedter and Olivier Mathieu

Received: 11 October 2022

Revised: 11 November 2022

Accepted: 29 December 2022

Published: 6 January 2023



Copyright: © 2023 by the authors. Licensee MDPI, Basel, Switzerland. This article is an open access article distributed under the terms and conditions of the Creative Commons Attribution (CC BY) license (<https://creativecommons.org/licenses/by/4.0/>).

1. Introduction

Polyoxymethylene dimethyl ethers (OME_{*n*}) are oligomers of structure CH₃O(CH₂O)_{*n*}CH₃ with chain length *n*. When OME_{3–5} are used as fuel, they suppress soot formation during combustion in internal combustion engines [1–7]. They can be produced from synthesis gas and methanol as either biofuel or Power-to-liquid (PtL) fuel. Thus, OME are promising and much discussed renewable synthetic fuels for a future sustainable and clean mobility [8–10]. Their physicochemical properties have been intensively studied in recent years; including vapor pressures [11,12], reaction kinetics [13,14], enthalpy model [1], and critical temperature [15]. Several insightful life cycle assessment (LCA) studies have shown OME_{*n*}'s reduction potential for CO₂ and local emissions [16–19]. Compared with the reference case of running a car on fossil diesel, the use of OME_{3–5} also reduces NO_x and soot emissions (43% and 25% respectively) disproportionately to the amount of fuel replaced with OME as a blend component [5–7].

OME_{3–5} is generally produced only from methanol. Parts of the methanol are converted to formaldehyde (FA), which is reacted with methanol to OME [20]. For the last step, there are two main classes of processes: (a) production of methylal (OME₁) or dimethyl ether and subsequent reaction with a water-free formaldehyde source, e.g., monomeric FA or trioxane [1,15,21,22], and (b) the direct synthesis from highly concentrated, methanolic FA solutions of low water content [20]. The latter process class (b) is tolerant to the presence of water (up to 0.1 g/g in the feed) [20] and generally requires fewer processing steps than processes of class (a) [23]. On the downside, water has to be removed in the same process in which OME is produced, which is challenging [20,22].

For any potential renewable fuel not yet on the market, studies on production cost are highly relevant and revealing. Therefore several studies on the cost of OME production

have been published. Schmitz et al. [24] calculated OME production cost for both routes as a function of the methanol cost through a very rough estimation of production costs based on analogies to refineries. However, they essentially neglected the challenging water removal in the formaldehyde concentration and the cost of formaldehyde production. Therefore, the results should be considered rather as a lower bound to the production cost.

Similarly, Burger and Hasse [25] reported the production cost of OME₃₋₅ as a function of the methanol cost. However, they did not describe how the result was obtained. Ouda et al. [26] report OME production cost of 805 EUR (converted from the original value of 951 USD) per ton of OME₃₋₅ at a small production capacity (35 kt per annum). However, the production process is based on the direct dehydrogenation of methanol to formaldehyde which is still fundamental research, and the cost estimate seems premature. Mantei et al. [10] present a very detailed study that gives the cost of production for OME from Power-to-X (PtX) hydrogen and CO₂ for four routes. They report the production cost of OME₃₋₅ as a function of the costs of hydrogen and CO₂. For the cost of hydrogen and CO₂ of 4241 EUR/t and 309 EUR/t, respectively, they reported the OME cost of 2382–2458 EUR/t. They concluded that ≥80% of the cost was related to raw material cost and that the production cost of OME only slightly varied among the four studied routes. Oyedun et al. [27] present production costs of 1.40–1.63 EUR/L (converted from the original values 1.66–1.93 USD/L) for OME for fuel blending produced from biomass. They use fixed raw material costs and a simplified OME production process for their assessment. They conclude that OME yield, capital cost, and biomass cost significantly influence OME cost and that the minimum OME cost can be obtained at a plant capacity of 4000 Mt/d [27]. Schemme et al. [28] present a study that gives the OME production cost when hydrogen is used as raw material for three different hydrogen costs, they use idealized assumptions on water removal in the formaldehyde concentration. For their base case of 4.6 EUR/kg_{H₂}, they report manufacturing costs of 1.85 EUR/L_{DE} for DME and 3.96 EUR/L_{DE} for OME, with the other investigated fuels ranging between the two [28].

All studies mentioned above have at least one of the following caveats: either they are very coarse estimates under strongly simplifying assumptions, e.g., formaldehyde production is essentially free of cost [24], or they report the cost depending on one single raw material, e.g., PtX hydrogen [10]. There is no study yet, that reports OME production cost as a function of the methanol cost and plant size based on a detailed, and thus meaningful, process model. Reporting OME production cost depending on the methanol cost is advantageous over reporting it for several individual raw materials upstream of methanol for the following reasons: First, there is an enormous market for methanol, and the OME price will therefore be tied to the methanol price for the foreseeable future. Second, the exclusion of the methanol production allows the flexible consideration of varying sources for said methanol; it could stem from CO₂ utilization, biomass, or fossil resources, the results for OME production cost hold. Third, this system boundary allows the assessment of a methanol production that is located somewhere where sustainable energy is cheap, while the OME production can be located anywhere, e.g., near the market for OME. In contrast to hydrogen or formaldehyde, methanol is liquid, stable, and easy to transport.

The present work has the objective to provide a techno-economic analysis and derive the OME cost as a function of a variable methanol cost. The costs of production for various plant sizes are determined. Multiple routes for the production and concentration of FA are analyzed and compared, including rather novel ones [29]. It is shown to what extent these process improvements have an influence on the production cost. The investigated processes are evaluated with process simulation, and heat integration is considered via a steam cycle. Techno-economic analysis, based on Towler [30] and Peters [31] is used to evaluate and report the capital and operational cost of all process steps.

2. Methodology

2.1. Description of Processes

2.1.1. Overview

Figure 1 gives an overview of the considered value-added chain. Raw materials are pure methanol, water, and air (21 vol% O₂, 79 vol% N₂). They are converted in three process steps to OME: FA production, FA concentration/water removal, and OME production. They enter the production at 25 °C. The intermediate product after the first two steps, which is fed to the last step, is a liquid mixture of formaldehyde and methanol (with a FA/ME mass ratio of 1.647 [13,20] and small amounts of water. This mixture is herein referred to as OME feedstock. Its water content should be as low as possible since water shifts the chemical equilibrium in the reactor to the educts and inhibits OME formation [13]. To the best of our knowledge, there is currently no industrial process to produce OME feedstock from methanol without producing large amounts of couple products such as aqueous FA solutions. We collected ideas from the patent literature for this task and conceptually designed 7 potential routes from methanol to OME feedstock without major side products, which are assessed and compared; cf. red horizontal arrows Figure 1. The routes differ in the combination of processes that are used for the steps of FA production and FA concentration/water removal. The combinations are comprised of seven different chemical processes (roman numerals I-VII), which are described in more detail in the next subchapters. One process might appear in several routes, e.g., processes I, II, III, IV, and VII. Note that Route 7 is special in that respect that it contains the special process VI, which combines the steps of FA production and FA concentration/water removal.

All side products and auxiliary materials (e.g., extracting agents) are preferably recovered as pure components and recycled. For comparison, all routes are scaled to produce the same mass flow rate of OME₃₋₅.

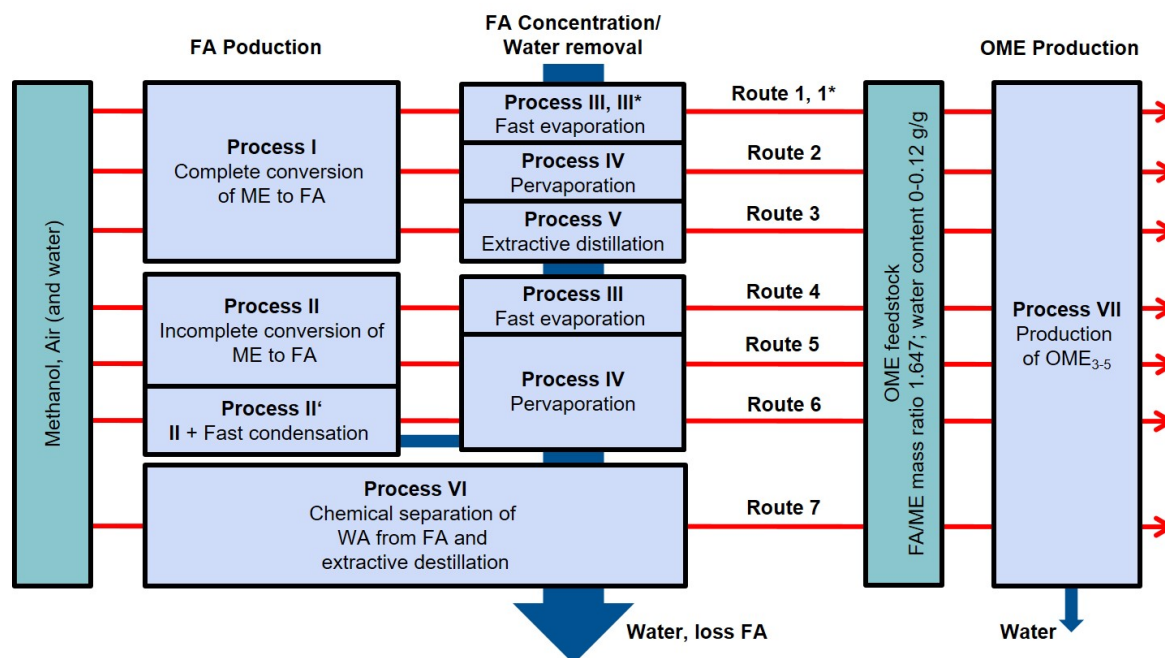
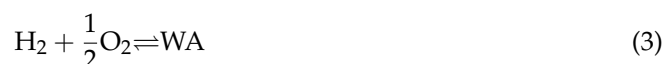
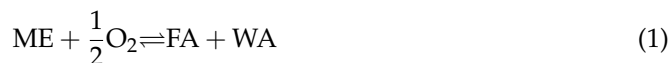


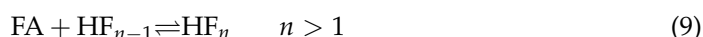
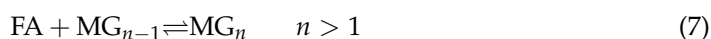
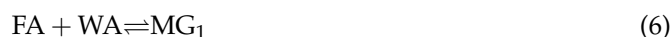
Figure 1. Overview of all considered processes in this work. Processes are numbered as follows. I: FA production that provides a 0.5 g/g FA–WA solution, herein the BASF process [32]. II: FA production with incomplete conversion [33]. III/III*: Separation of FA solutions in a fast evaporator or column [10,29] (Routes 1 and 1* differ only in the type of fast evaporation process, i.e., either III or III*). IV: Pervaporation to remove water from FA solutions [34,35]. V: Extractive distillation of FA solutions [36]. II': FA production with incomplete conversion and fast condensation of water from reactor product [37]. VI: Production of Methylal and separation of water, oxidation of MAL to FA and following extractive distillation [38]. VII: OME production adopted from Schmitz et al. [20].

2.1.2. Formaldehyde Production

Processes to produce FA solutions are established in the industry. Generally, methanol is reacted with oxygen (in air) over silver or metal-oxide catalysts to FA, WA, H₂, CO, and CO₂ [10,39].



Two process types are distinguished: Process I yields complete ME conversion in one pass through the reactor (e.g., Formox processes, off-gas recycle processes). The reactor delivers a mixture of FA and WA with very little ME (0–2 wt%). Many such processes are used in industry; herein, we chose the BASF process for producing a 0.5 g/g aqueous FA solution as described in Ullmann's Encyclopedia of Industrial Chemistry [32]. Process II operates with incomplete ME conversion in one pass; here, the reactor delivers mixtures of FA, ME, and WA with a distinctly higher FA/WA ratio than in process I [32]. In process II, there is usually subsequent removal and recycling of ME from the reactor product to achieve complete conversion of ME. However, this is not needed for our purpose. Process II is appealing for the production of methanolic formaldehyde solution because the reactor product already contains less water per unit of FA than in processes with complete conversion. We use data from Vancells [33] for process II. In a variation of process II, process II', part of the reactor product is rapidly condensed to further reduce the water content [37]. In all state-of-the-art processes, FA is produced in a gas phase reactor and afterward chemically absorbed in water or methanol. Thereby, formaldehyde reacts with water and methanol to poly(oxymethylene) glycols (MG_n, HO-(CH₂O)_n-H) and poly(oxymethylene) hemiformals (HF_n, HO-(CH₂O)_n-CH₃), respectively, [40].



These reactions occur at a considerable rate even without the presence of catalysts, resulting in a complex reactive phase behavior of FA solutions, which makes it challenging to remove water and produce OME feedstock. It is, for example, not possible to use simple distillation columns to remove large quantities of water [41].

2.1.3. Formaldehyde Concentration

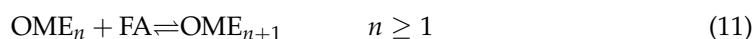
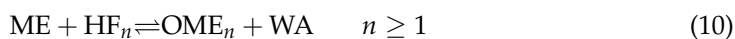
In routes 1–6, water must be removed from the FA solutions provided by an FA process of type I or II. Three different technologies are considered for this purpose. First, highly concentrated FA solutions are typically produced in fall-film evaporators or thin-film evaporators [42–44]. This option is considered as Process III/III* in Figure 1. Process III has been developed in our group [29] and combines thin-film evaporation with a distillation column to recover FA and minimize FA losses. Process III* is a simpler scheme adopted from Mantei et al. [10] to enable comparisons with their results. It uses two thin-film evaporators in series without formaldehyde recovery. It has, therefore, FA losses of up to 8% in effluent water [10]. Besides evaporation, we also consider two alternative technologies: Process IV is a membrane separation of water from FA solutions; the chosen reference process employs pervaporation [34,35]. Process V is based on the extractive distillation of aqueous FA solu-

tions to obtain concentrated gaseous FA, which is dissolved in methanol subsequently [36]. We added a FA concentration column for formaldehyde recovery from the effluent water in process V. In Route 7, Process VI combines FA production and concentration. FA is reacted to methylal (MAL) before water is removed. MAL is then oxidized to FA, and pure gaseous FA is obtained in subsequent extractive distillation [38]. The FA is then dissolved in ME to obtain OME feedstock.

The main difference between the routes lies in the FA concentration/water removal technology. However, the upstream FA production in Routes 1–6 also influences the overall performance: It significantly influences carbon losses via the FA reactor's selectivity. Further, Route 1–7 lead to OME feedstock of different water content. This influences the efficiency of the OME process, which was explicitly considered in the assessment.

2.1.4. Ome Production

The process presented by Schmitz et al. [20] is adopted without modification (Process VII). Simulation data [20] and a demonstration plant exist [45]. The process converts OME feedstock to OME_{3–5} and water over an acidic solid catalyst, ion exchange resin Amberlyst 46. OME are formed from ME and FA and the respective HF_{*n*}.



The reactor effluent is separated in a direct distillation sequence in three fractions: (1) light OME, ME, FA, WA; (2) product OME_{3–5}; (3) heavy OME. Water is separated from (1) using a pervaporation unit before it is recycled with fraction (3) to the reactor.

2.1.5. Detailed Descriptions

All processes and the basic apparatus designs are adopted from the corresponding sources indicated in the caption of Figure 1. Process flow diagrams of all processes and detailed descriptions are given in the Supplementary Materials. Consistent material balances are derived from the simulations performed in the present work; the required information is adopted from the original literature as described in the Supplementary Materials.

2.2. Process Simulation

The processes I–VII are simulated as steady-state processes in the software Aspen Plus V8.8. Aspen Process Economic Analyzer is used for equipment sizing.

2.2.1. Property Model

For processes I–VII, we adopt an activity-based fluid phase equilibrium model for the components FA, WA, ME, HF₁–HF₂ and MG₁–MG₂ from Kuhnert et al. [46]. For thin-film evaporators, the reaction kinetics in the liquid phase are modeled as described by Ott et al. [47]. For the noncondensable gases N₂, O₂, CO, CO₂, H₂, property data for vapor pressures, enthalpies of formation in the gas phase, enthalpies of vaporization, ideal gas heat capacities are adopted from the DIPPR database [48]. Gas solubilities are neglected for these components. For process VII, we adopt the activity-based fluid phase equilibrium and reactor model from Schmitz et al. [49], which is slightly different from the one used in I–VI. Details are given in the Supplementary Materials. We have not found a consistent enthalpy model for the given chemical system in the literature, so we set one up as follows.

Neglecting excess enthalpies, the enthalpy streams are calculated to

$$\dot{H}_{\text{stream}} = \sum_{i=1}^K \dot{m}_i h_i(T_{\text{stream}}). \quad (12)$$

where K is the number of components in the stream, \dot{m}_i is the mass flow rate of the i -th component and $h_i(T_{\text{stream}})$ the specific enthalpy of the pure component i at the physical state

of the stream. The specific enthalpies at temperature T_{stream} are normalized to the enthalpy of formation $h_i^f(T^\theta)$ in the gaseous state at standard temperature T^θ for gaseous streams:

$$h_i(T_{\text{stream}}) = h_i^f(T^\theta) + \int_{T^\theta}^{T_{\text{stream}}} c_{p,i}^g dT, \quad (13)$$

and for liquid streams:

$$h_i(T_{\text{stream}}) = h_i^f(T^\theta) + \int_{T^\theta}^{T_{\text{stream}}} c_{p,i}^g dT - \Delta h_{v,i}(T_{\text{stream}}). \quad (14)$$

The pressure dependence of the enthalpies is neglected. $c_{p,i}^l$ and $c_{p,i}^v$ are the isobaric, specific heat capacities in the liquid and vapor phase, respectively. $\Delta h_{v,i}$ denotes the enthalpy of vaporization. The details on the used correlations for the mentioned quantities are given in the Supplementary Materials.

2.2.2. Unit Modeling and Design

Heat duties of all units are derived from the process simulations performed in the present work. The equipment cost calculation requires the respective cost determining factors for each unit given in Table 1.

Table 1. Cost determining factors for each unit for the techno-economic analysis.

Unit	Cost Determining Factors
Distillation columns, absorbers	Column height and diameter, Column internals: Trays/Packing
Reactors	Heat duty, Catalyst mass
Heat exchangers, evaporators, condensers, Thin-film-evaporators, Off-gas-burners	Heat exchange area
Membrane units	Membrane surface area

The units are modeled as follows:

- Distillation and absorption columns: All columns are simulated using the equilibrium stage model, assuming physical equilibrium and chemical equilibrium considering Reactions (6)–(9) on all stages. For distillation columns, the condenser (=total condenser) and reboiler are modeled with one additional stage, respectively. The pressure drop along the column is neglected. If not given in the reference, the stage numbers are chosen so that 1.2 times the minimum required reboiler heat duty is used. The feed stage is found using the built-in feed stage optimization of Aspen Plus. The remaining two degrees of freedom per column were fixed by the specification of top and bottom product concentrations as given in the original source; the corresponding concentrations are highlighted in the respective stream tables as bold (cf. Supplementary Materials). The extractive distillation columns in processes V and VI were not modeled with an equilibrium stage model because of missing property data (for extraction agents). Instead, the minimum reflux ratio is calculated based on Underwood's Equation [50] and is used to estimate the approximate heat duties, cf. Supplementary Materials. For these extractive distillation columns, height and diameter are adopted from the original work. For all other columns, height and diameter are estimated with the Aspen Process Economic Analyzer, both packed and trayed columns are sized with the default option as DTW Tower.
- Reactors: Reactor product compositions, conversion and selectivity are adopted from the original source. The heat duty \dot{Q} is calculated via the energy balance:

$$\dot{Q} = \dot{H}_{\text{out}} - \dot{H}_{\text{in}} \quad (15)$$

Reactor cost is based on \dot{Q} and the temperature level; no further design was done.

- Heat exchangers, condensers, evaporators: Heat is generally provided via a steam network operating at the pressure stages given in Table 2. The water condensate leaves the heat exchanger at the same temperature as the steam entered. Cooling is done preferably by producing steam at the maximum pressure level. Low temperature (LT) cooling is done using the media listed in Table 2. Cooling demand at temperatures above 40 °C is realized via cooling water, which enters the heat exchanger at 25 °C and leaves it at a maximum of 60 °C. Cooling below 40 °C requires different cooling mediums at an increased cost. Ammonia and salt solutions were only used for condensation at a constant temperature. Using the mean logarithmic temperature difference and the respective heat transfer coefficient for the heat exchanger type (cf. Supplementary Materials) the area of the heat exchanger is determined.

$$A = \frac{\dot{Q}}{k * \Delta T_{\text{mean}}} \quad (16)$$

The steam level and cooling media are chosen so that a minimum temperature difference of 10 K [50] throughout the heat exchanger is not undercut. Heat integration along the process chain from ME to OME is realized via the steam network. Heat below 160 °C is not considered for steam generation, therefore, not considered for heat integration unless stated otherwise in the process description. Note that it is likely possible to use part of this excess heat to supply district heat, but this depends on the boundary conditions of the plant and is not further considered here.

- Thin film evaporators (TFEs) and other kinetic separators: Fast evaporation of aqueous and methanolic FA solutions results in a reactive phase equilibrium that does not reach the chemical equilibrium. These units are modeled as open evaporation with multiple stages considering the vapor-liquid equilibrium and the reaction kinetics of reactions (6)–(9) [47] on every stage. Details on the model are given in our previous work [29].
- Pervaporation: The primary energy demand for pervaporation results from the permeate's phase change and is calculated from its heat of vaporization. The membrane surface area is calculated based on the correlation given by Schmitz et al. [34] from the given output stream's specification.

Table 2. First part: Pressure stages and temperatures of the employed steam network; second part: Temperatures of the cooling media and the process stream.

Steam Network Pressure Levels			
	T_{Steam}	$T_{\text{out}}^{\text{Stream}} / ^\circ\text{C}$ (consumption)	$T_{\text{out}}^{\text{Stream}} / ^\circ\text{C}$ (production)
Steam 40 bar	290	280	300
Steam 20 bar	220	210	230
Steam 4 bar	150	140	160
LT Cooling Media			
Cooling Medium	$T_{\text{min}}^{\text{Product}} / ^\circ\text{C}$	$T_{\text{in}}^{\text{Medium}} / ^\circ\text{C}$	$T_{\text{out(max)}}^{\text{Medium}} / ^\circ\text{C}$
Cooling water	40	25	60
Chilled water	20	10	60
Ammonia	10	0	0
Salt solutions	−5	−15	−15
Salt solutions	−10	−20	−20

Pumps are not explicitly sized; they are considered using the factor model in the economic analysis. Burners are modeled like reactors with ascribed heat exchangers but are based on a different cost correlation.

2.3. Process Economics

Capital expenditure (CAPEX) and operational expenditure (OPEX) are estimated using an equipment factored estimating method for each route. The cost determining factors of the main process equipment is determined based on the simulation results, and subsequently, the purchasing cost for each item is retrieved. For standard equipment, e.g., heat exchangers or columns, cost equations have been adopted from Towler and Sinnott [30], and Peters and Timmerhaus [31]. All purchasing costs have been updated for the year 2018 using the Chemical Engineering Plant Cost Index (CEPCI). Costs in US Dollars have been converted using the average exchange rate of 0.85 EUR/USD in 2018 and a location factor of 1.11 for Germany [30].

The purchasing costs are multiplied by cost factors accounting for additional charges, e.g., installation, power supply, engineering. For this study, cost factors have been taken from Peters and Timmerhaus [31]. A detailed overview of the applied cost factors is given in the Supplementary Materials. The working capital is estimated as 15% of the total capital investment. A plant lifetime of 20 years is assumed with a Weighted Average Cost of Capital (WACC) of 5%, resulting in a capital charge factor of 0.08, which is used to calculate the annuity.

Indirect OPEX costs are determined using factors from Peters and Timmerhaus [31]. Distribution and R&D costs are neglected to only account for costs directly linked to the production. The direct OPEX is calculated based on the material and energy balances of the process. It is assumed that generated steam can be sold for the same price as the buying costs. Steam and cooling costs vary depending on the steam pressure level and the employed cooling medium, cf. Table 3.

Table 3. Steam and cooling cost depending on steam pressure level and employed cooling medium.

Pressure Level	Cost/Credit/EUR/t
Steam 40 bar	23.5
Steam 20 bar	23.1
Steam 4 bar	22.8
Cooling Medium	Cost/EUR/kWh
Cooling water	0.005
Chilled water	0.0075
Ammonia	0.015
Salt solutions	0.02
Salt solutions	0.025

The labor costs are estimated based on Towler and Sinnott [30]. Three shift positions are assumed for a continuous fluid processing plant at a large site. To account for vacations and other employee absences, 4.5 shifts are assumed. This results in 13.5 operation positions with a working time of 37 h per week. A detailed overview of all considered OPEX factors and raw material costs, utility costs, and labor costs is given in the Supplementary Materials. The levelized product cost (LPC), including annuity on CAPEX and all OPEX, is calculated per t of produced OME. A plant size of 100 kt OME production per year and a methanol cost of 401 EUR/t (average price Methanex 2018) are assumed as the base case. Variations of plant size and methanol cost are also considered.

The achieved cost estimates for the CAPEX are categorized as class 4 estimates by the American Association of Cost Engineering (AACE) International and usually provide a relative uncertainty of $\pm 30\%$ [51]. The uncertainty in the levelized product cost for OME is smaller, as the current methanol cost is an input parameter. It follows as

$$\text{Rel.Uncertainty(LPC)} = \pm 30\% \left(1 - \frac{\text{Raw material cost}}{\text{Total cost of production}} \right). \quad (17)$$

3. Results and Discussion

3.1. Material Balances

Detailed stream tables for all processes are given in the Supplementary Materials. Key performance indicators are given in Table 4. The carbon yield is defined as the amount of carbon atoms in the product divided by all carbon atoms entering the process. The heat demand is the sum of the net heat demands from the steam network on all three pressure levels.

Table 4. Key results for all routes for a plant size of 100 kt OME production per year and a methanol price of 401 EUR/t. The standard deviation is given in the last column to indicate the size of the occurring differences in a KPI. However, one should keep in mind that the routes are based on different technologies when comparing them directly.

Route	1	1*	2	3	4	5	6	7	σ
Carbon yield/mol/mol	0.935	0.881	0.927	0.925	0.817	0.812	0.928	0.926	0.05
Heat demand/GJ/t OME	6.18	5.05	3.36	13.36	2.51	−1.11	6.57	8.70	4.05
CAPEX/Mio EUR	32.39	28.32	24.66	27.80	31.83	23.34	28.66	27.18	2.92
OPEX/Mio EUR/a	57.66	59.32	53.46	68.63	62.40	54.57	48.23	64.63	6.15
LPC/EUR/t OME	597.26	611.3	550.31	704.13	644.41	560.43	500.69	662.98	61.94

All routes perform similarly regarding carbon yield. There are rather small carbon losses in all routes because the dilute FA solutions are usually concentrated and recycled for maximum utilization. Therefore, the carbon yield is mainly determined by the yield of the FA plant and the FA reactor's selectivity. Consequently, routes with the same FA process (1–3, 4–5) have similar carbon yields among them. Routes 1–3, as well as routes 6 and 7, lead to approximately 0.93 mol/mol carbon yield. Routes 4 and 5 have a lower yield of 0.82 mol/mol due to a lower selectivity in the respective FA reactor. Route 1* is an exception and has significant losses in the FA concentration process. Despite the same FA production process as Routes 1–3, it leads to a carbon yield of 0.88 mol/mol, 0.05 mol/mol lower. The carbon losses in the OME process are negligible for all routes.

3.2. Energy Balance

Detailed tables of the energy balances for single units with respective temperature levels are given in the Supplementary Materials. Table 4 and Figure 2 show the overall heat demand per t OME from the steam network and the heat demand and excess per t OME at the respective temperature levels for the base case. Excess is displayed as a negative bar, demand as a positive bar. It shows the net heat demand at the steam levels 40, 20, and 4 bar (steam production and consumption) for all routes. Heat is integrated within every pressure level via the steam network, but not to lower pressure levels, as this would destroy exergy. LT cooling has to be provided at low temperatures below 25 °C.

Due to the exothermic oxidation of methanol to formaldehyde, all routes provide large amounts of excess heat. For routes 1, 2, 4, 5, and 6, this excess heat would suffice to provide all required heat input in the FA production and concentration step. Furthermore, routes 2, 4, and 5 provide usable excess heat that can be integrated into the OME process via the steam network. Routes 3 and 7 have a higher heat demand; they require more heating and provide no excess heat for the OME process. Route 1* has a very similar heat demand to Route 1, but the heat demand is at a lower temperature level.

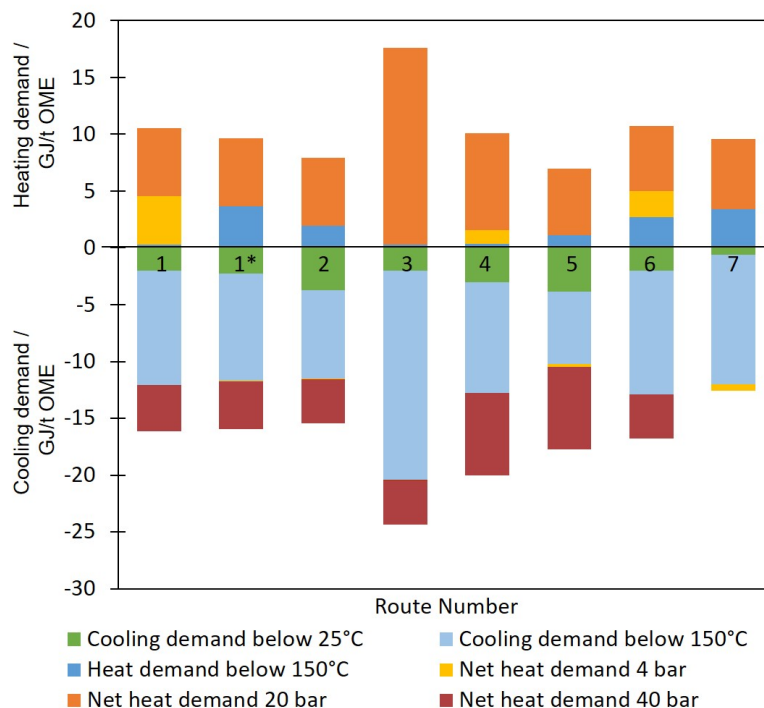


Figure 2. Net heat demand per t OME at every steam level (40, 20, 4 bar) for all routes. Excess heat is negative, heat demand positive.

3.3. Economics

3.3.1. Base Case

Equipment cost:

Figure 3 gives the estimated equipment costs of all routes for a plant of 100 kt OME production per year. The costs are broken down by equipment type. The most significant cost contributors are heat exchangers, distillation columns, and evaporators. The equipment costs in the OME process mainly stem from the two distillation columns. The estimated equipment costs for FA production and concentration vary widely between the investigated routes 1–7, from 3.9 (Route 2) to 5.8 Mio (Route 1) EUR. Considering that CAPEX costs occur at the beginning of the project and constitute the capital at risk over time, the financial risk differs significantly between the process options.

Routes 1, 1*, and 4 have high equipment costs, primarily due to the expensive thin-film evaporators. Routes 3, 6, and 7 have moderate costs. Their largest cost contributors are distillation columns and a large number of unit operations. Membrane units like they appear in Routes 2 and 5 have only a small contribution to the overall cost, making these routes cheap options. However, the high uncertainty regarding the membrane costs should be considered, and the membrane material has been treated as a consumable only considered in the OPEX. Despite its large number of units, Route 7 has a relatively low total equipment cost. The discussed differences in the equipment costs between the routes are correspondingly pronounced in the total CAPEX, cf. Table 4.

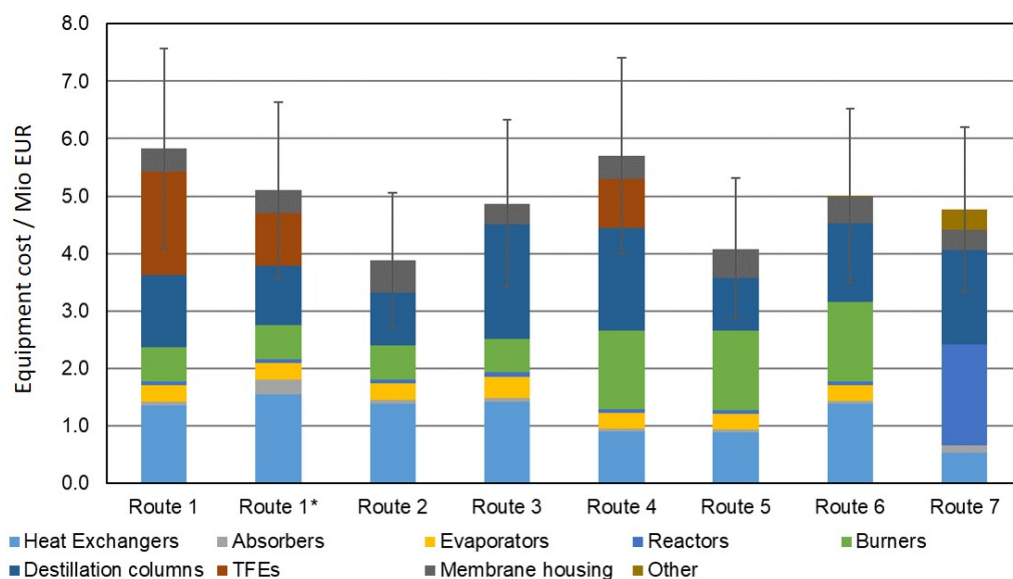


Figure 3. Equipment cost of all Routes for a plant size of 100 kt OME/a. The whiskers show the uncertainty in the total equipment cost for each route ($\pm 30\%$ [51]).

Operational cost:

Figure 4 and Table 4 show the OPEX for a plant size of 100 kt OME per year and a methanol price of 401 EUR/t. It ranges from 48.2 (Route 6) to 68.6 (Route 3) Mio EUR per year for the routes.

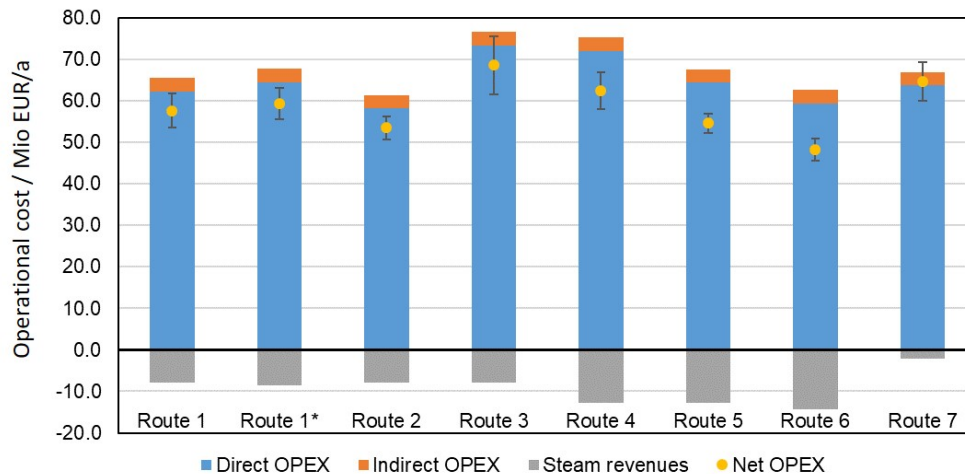


Figure 4. Operational cost/a of all routes for a plant size of 100 kt OME/a. The whiskers show the uncertainty in the operational costs.

The variance in the OPEX is less noticeable than in the CAPEX; this is mainly because the raw material costs cause nearly two-thirds of the entire OPEX. Raw material costs are followed by indirect OPEX cost, which summarizes several smaller indirect cost contributors and the operating labor cost. The differences between the routes arise from the differing carbon yields, utility consumptions, and potentials for steam generation. Routes 3, 4, and 7 show the highest OPEX. In Routes 3 and 7, this is due to high heat demand and a lack of significant steam revenue; in Route 4 due to carbon losses in the FA process. Routes 2, 5, and 6 show a low OPEX due to the low costs for the employed pervaporation units. Note that membrane material replacement only accounts for 0.6% of the OPEX cost. Route 1* has a slightly higher OPEX than Route 1 due to its higher carbon losses. For all routes, the annuity of the CAPEX only contributes around 4% to the manufacturing cost; the OPEX

has a much larger share. This is partly caused by the rather low WACC and long plant lifetimes that were assumed, while this seems striking, comparable studies result in similar proportions of OPEX and CAPEX [10,28].

3.3.2. Sensitivity Studies: Manufacturing Cost for OME

The levelized product cost for OME was analyzed for variations of methanol cost and plant size in sensitivity studies. The LPC as a function of the methanol cost is shown for all routes in Figure 5. We also calculated an average value for the LPC for a plant size of 100 kt OME₃₋₅/a. Based on the mean incline and mean y-intercept of all routes, it is:

$$\text{LPC}_{\text{OME}} = 79.07 \text{ EUR/t} + 1.31 * c_{\text{Methanol}} (\text{EUR/t}) \quad (18)$$

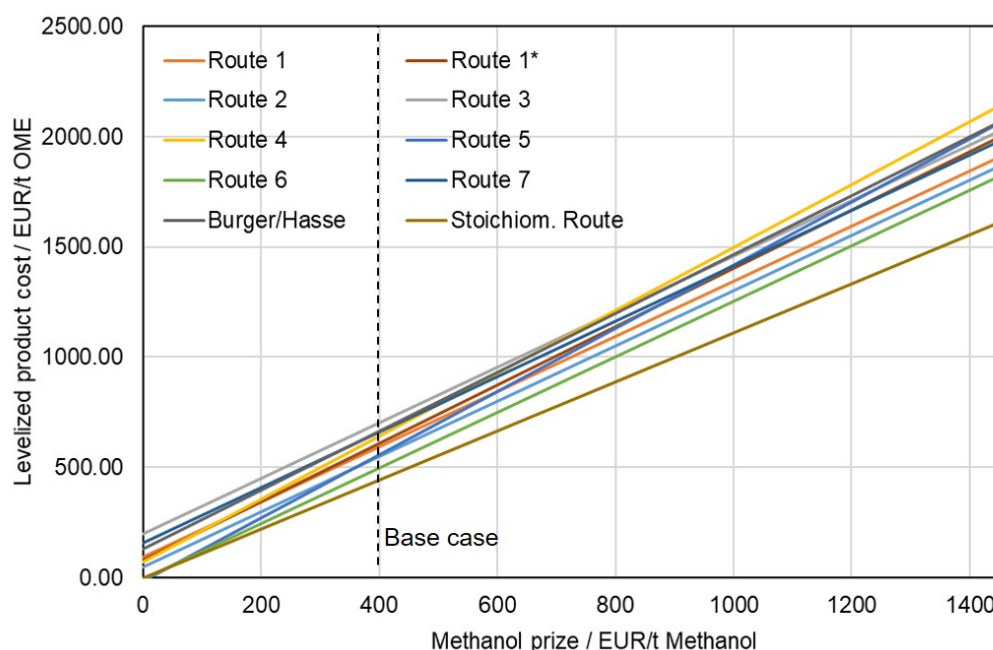


Figure 5. Levelized product cost per t OME for all routes as a function of the methanol cost for a plant size of 100 kt/a.

Further, the minimum feasible manufacturing cost for OME ($c_{\text{OME}}^{\text{min}}$) is calculated based solely on the methanol cost and the stoichiometrically required methanol for the production of 1 t of OME (cf. Reactions (10) to (11)).

$$c_{\text{OME}}^{\text{min}} = 1.112 * c_{\text{Methanol}} (\text{EUR/t}) \quad (19)$$

In order to better differentiate between routes, the minimum feasible manufacturing cost is subtracted from the LPC for routes 1 to 7. This yields the process-dependent cost ($c_{\text{OME}}^{\text{PD}}$), cf. Figure 6.

The y-intercept at 0 EUR/t methanol is determined by the fixed cost of the route, and the slope by its carbon yield. OME production via routes 2 and 6 is the cheapest for methanol costs higher than 350 EUR/t; both routes have a high carbon yield and low CAPEX and OPEX, and both routes employ pervaporation. Route 5 also employs pervaporation and has low costs for low ME costs, but the high carbon losses in the FA process II lead to high manufacturing costs for higher ME costs. Routes with considerable carbon losses, i.e., Routes 4 and 5 via their lower FA reactor selectivity and Route 1* via the FA losses in the concentration process, show a larger slope. Therefore, they become less competitive with higher methanol costs. For lower ME costs, they perform reasonably well. Route 3 leads to the highest manufacturing cost for ME costs lower than 700 EUR/t. For

higher costs, it is more economical than Routes 4 and 5 due to their significant carbon losses. Routes 1 and 7 both lead to mid-range costs for all methanol costs. Routes employing pervaporation generally lead to the lowest costs for all ME costs over 300 EUR/t, due to their low carbon losses and energy consumption. Routes employing extractive distillation lead to high cost for all ME cost, and should probably only be used if highly pure FA is required. Thin-film evaporation performs well in if no FA is lost in side products.

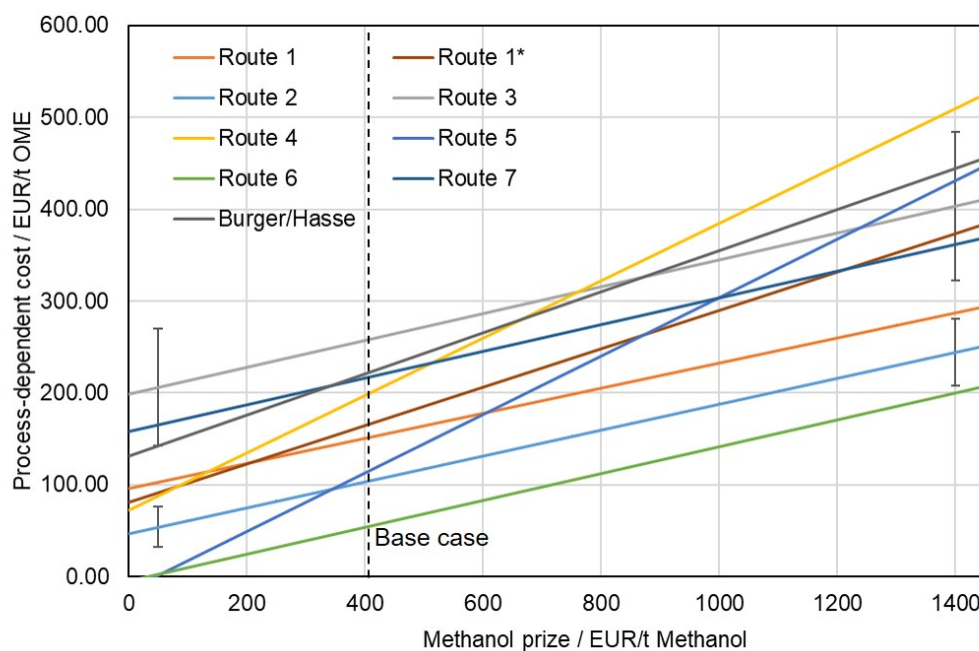


Figure 6. Process-dependent cost per t OME for all routes as a function of the methanol cost for a plant size of 100 kt/a.

One should consider the significant uncertainty in the equipment cost estimation and that all graphs are close together. The uncertainty is less pronounced in the LPC due to the large share of the ME cost but is still significant ($\pm 30\%$ to $\pm 1.5\%$, depending on route and methanol cost). In Figure 6, where a large share of the methanol cost is already deducted, the uncertainty grows again. To visualize the size of the uncertainty, it is shown for Route 2 (smallest uncertainty) and route 5 (largest uncertainty) for the methanol cost of 50 and 1400 EUR/t. For the base case (methanol costs of 401 EUR/t), the uncertainty is between $\pm 5\%$ to $\pm 10\%$, depending on the route.

For this cost, the OME manufacturing cost range between 586 and 821 EUR/t. These results are in good agreement with other publications that analyze comparable routes. Burger and Hasse [25] give OME cost of 668 EUR/t for methanol costs of 401 EUR/t. Their results are also shown in Figure 5 and 6 for other methanol costs. Schmitz et al. give OME costs of 522 EUR/t for methanol costs of 255 EUR/t. For these methanol costs, our study results in slightly lower OME costs of 310 to 513 EUR/t. This is mainly due to lower carbon losses in the FA production and steam revenues. Compared with Route 1*, which was suggested by Mantel et al., the improved thin-film evaporation in Route 1 saves 2.3% on the manufacturing cost for a methanol price of 401 EUR/t. For higher ME costs of up to 1500 EUR/t, these savings rise to 4.7%, while these savings are within the uncertainty, they result solely from the material balance, which is much less uncertain. Since the carbon yield has the most significant influence on the cost, all new production processes should aim to increase the yield in the FA reactor and reduce losses of FA and methanol in the subsequent concentration.

The influence of the plant size on the levelized product cost is also investigated in a sensitivity study for all routes. Figure 7 gives the results for the fixed methanol cost of 401 EUR/t.

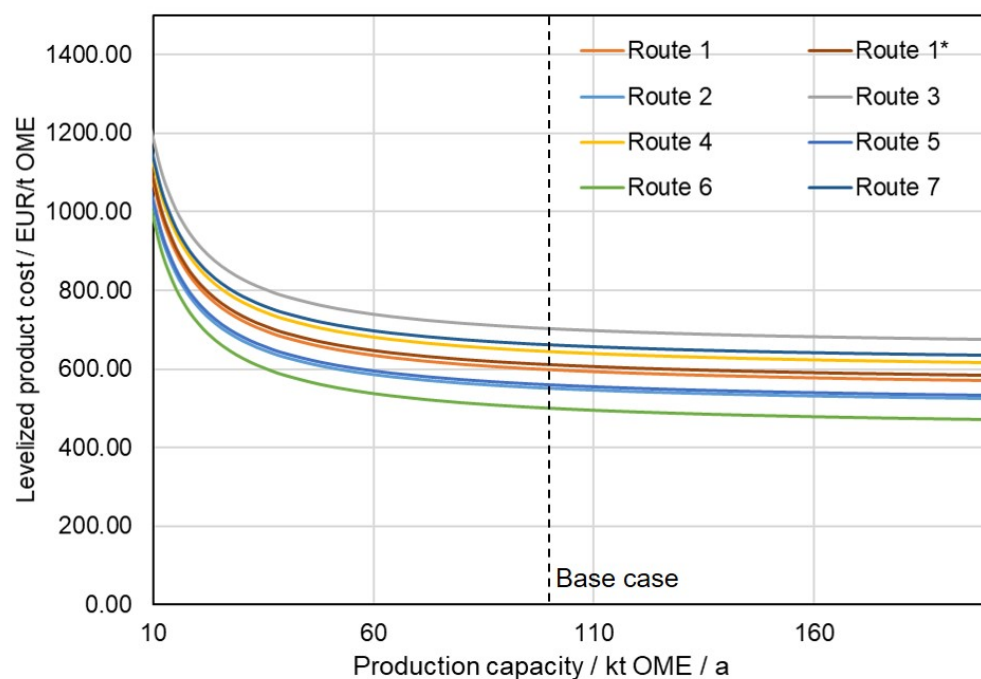


Figure 7. Levelized product cost per t OME for all routes as a function of the plant size for a ME cost of 401 EUR/t.

The levelized product cost increases drastically with smaller plant sizes for all routes. Below production capacities of 50,000 tons OME per year, the cost increase strongly. For larger production capacities, the raw material cost dominates all other cost contributors. The discussed differences between the routes hold for all plant sizes. However, note that the scale-up is simplified; it considers the increased cost via the unit size used as input for the cost correlation by Towler and Sinnott [30].

While this study achieves very good agreement with comparable works, there are some limitations to consider. First, the uncertainty stemming from the employed techno-economic has to be considered when evaluating the cost. Second, some aspects of the investigated technologies were deemed beyond the scope. The removal of wastewater was not considered here, while the removed wastewater is quite pure, it may cause further costs for some routes, which might not be negligible. Further, we assumed that all carbon should be converted to OME. Joint products could lead to lower production costs for OME. Of course, the involved processes could be improved further. For instance, the FA reactor could be trimmed toward hydrogen recovery. There is also the possibility to use methanol or wastewater as an absorbent in the FA absorber, which could lower the water content of FA solutions [52]. Although these options were not considered in the present work, major cost reductions seem unlikely as the levelized product cost is determined mainly by the methanol cost.

4. Conclusions

Several routes for OME production from methanol via the water-tolerant OME process were investigated. Different technologies for removing water from formaldehyde solutions were evaluated, simulated, and compared. Techno-economic analysis was used to calculate the manufacturing cost of OME as a function of the methanol cost and plant size. Key performance indicators were identified, and all routes were compared. For a current methanol market cost of 401 EUR/t, the levelized product cost of OME range between 586 and 821 EUR/t. The routes using pervaporation result in the lowest levelized product cost for all methanol costs higher than 300 EUR/t. They have high carbon yields and low energy and investment costs. Routes that rely on extractive distillation result in high OME

costs. For methanol costs up to 350 EUR/t, they result in the highest levelized product costs. For higher methanol costs, the routes with the highest carbon losses, based on one of the FA plants with incomplete conversion, become even more expensive. Processes based on pervaporation perform well, but there are still questions regarding the long-term stability of the membrane, and there is high uncertainty in the membrane cost. Thin-film evaporation performs reasonably well when combined with distillation for maximum FA recovery. Extractive distillation is not recommended unless highly pure FA is required. The most influential parameter on the performance of any route is the carbon yield. Thus, for OME production, the selectivity in the FA production process should be maximized, and the FA losses in the subsequent concentration and OME production should be minimized.

Supplementary Materials: The following supporting information can be downloaded at: www.mdpi.com/xxx/s1. Techno-economic analysis of large scale production of poly(oxymethylene) dimethyl ether fuels from methanol in water-tolerant processes.

Author Contributions: Conceptualization, Y.T. and V.D.; methodology, Y.T. and V.D.; investigation, Y.T. and V.D.; resources, H.S. and J.B.; writing—original draft preparation, Y.T. and J.B.; writing—review and editing, Y.T.; supervision and project administration S.F. and J.B.; funding acquisition, H.S. and J.B. All authors have read and agreed to the published version of the manuscript.

Funding: This study was carried out in the framework of the E2Fuels project (project no.: 03EIV011G) funded by the German Federal Ministry for Economic Affairs and Energy. The financial support is gratefully acknowledged.

Data Availability Statement: All data used in this work is reported within the manuscript text and the Supplementary Materials.

Acknowledgments: The authors acknowledge the cooperation within the Network TUM.Hydrogen and PtX.

Conflicts of Interest: The authors declare no conflict of interest.

Abbreviations

The following abbreviations and variables are used in this manuscript:

Abbreviations

C	Column
CAPEX	Capital Expenditure
CEPCI	Chemical Engineering Plant Cost Index
DE	Diesel equivalent
DME	Dimethylether
E	Various unit operations with phase change
EUR	Euro
FA	Formaldehyde
HF _n	Poly(oxymethylene) hemiformal
HX	Heat exchanger
LPC	Levelized product cost
MAL	Methylal
ME	Methanol
MG _n	Poly(oxymethylene) glycol
OME _n	Poly(oxymethylene) dimethyl ether of chain length n
OP	Operating point
OPEX	Operational Expenditure
RR	Reflux Ratio
TFE	Thin Film Evaporator
TRI	Trioxane
TRL	Technology Readiness Level
USD	US Dollar

VLE	Vapor-liquid equilibrium
WA	Water
WACC	Weighted Average Cost of Capital
Variables	
A	Surface
c	Cost
c_p	Isobaric heat capacity
$\Delta h_{v,i}$	Enthalpy of vaporization
$\Delta h_{R,i}$	Reaction enthalpy
H	Enthalpy
h_i	Specific enthalpy of component i
h_i^f	Standard enthalpy of formation of component i
K	Number of components
k	Heat transfer coefficient
\dot{m}	Mass flow rate
N	Number of stages
n	Chain length
p	pressure
\dot{Q}_i	Heat duty of unit i
\dot{Q}_{tot}	Total heat duty
R	Universal gas constant
T	Temperature
T_c	Critical temperature
x_i^k	Mass fraction of component i in k

References

- Burger, J.; Siegert, M.; Ströfer, E.; Hasse, H. Poly(oxyethylene) dimethyl ethers as components of tailored diesel fuel: Properties, synthesis and purification concepts. *Fuel* **2010**, *89*, 3315–3319. [[CrossRef](#)]
- Lumpp, B.; Rothe, D.; Pastötter, C.; Lämmermann, R.; Jacob, E. Oxymethylene ethers as diesel fuel additives of the future. *MTZ Worldw. eMagazine* **2011**, *72*, 34–38. [[CrossRef](#)]
- Zhang, Q.; Wang, W.; Zhang, Z.; Han, Y.; Tan, Y. Low-Temperature Oxidation of Dimethyl Ether to Polyoxymethylene Dimethyl Ethers over CNT-Supported Rhenium Catalyst. *Catalysts* **2016**, *6*, 43. [[CrossRef](#)]
- Baranowski, C.J.; Bahmanpour, A.M.; Kröcher, O. Catalytic synthesis of polyoxymethylene dimethyl ethers (OME): A review. *Appl. Catal. B Environ.* **2017**, *217*, 407–420. [[CrossRef](#)]
- Härtl, M.; Seidenspinner, P.; Jacob, E.; Wachtmeister, G. Oxygenate screening on a heavy-duty diesel engine and emission characteristics of highly oxygenated oxymethylene ether fuel OME1. *Fuel* **2015**, *153*, 328–335. [[CrossRef](#)]
- Pélerin, D.; Gaukel, K.; Härtl, M.; Wachtmeister, G. Simplifying of the Fuel Injection System and lowest Emissions with the alternative Diesel Fuel Oxymethylene Ether. In Proceedings of the 16th Conference: The Working Process of the Internal Combustion Engine, Graz, Austria, 28–29 September 2017.
- Pélerin, D.; Gaukel, K.; Härtl, M.; Wachtmeister, G. Recent results of the sootless Diesel fuel oxymethylene ether. In Proceedings of the International Motor Congress, Baden-Baden, Germany, 21–22 February 2017; pp. 439–456. [[CrossRef](#)]
- Schemme, S.; Samsun, R.C.; Peters, R.; Stolten, D. Power-to-fuel as a key to sustainable transport systems - An analysis of diesel fuels produced from CO₂ and renewable electricity. *Fuel* **2017**, *205*, 198–221. [[CrossRef](#)]
- Burre, J.; Bongartz, D.; Deutz, S.; Mebrahtu, C.; Osterthun, O.; Sun, R.; Völker, S.; Bardow, A.; Klankermayer, J.; Palkovits, R.; et al. Comparing pathways for electricity-based production of dimethoxymethane as a sustainable fuel. *Energy Environ. Sci.* **2021**, *14*, 3686–3699. [[CrossRef](#)]
- Mantei, F.; Ali, R.E.; Baensch, C.; Voelker, S.; Haltenort, P.; Burger, J.; Dietrich, R.U.; Von Der Assen, N.; Schaadt, A.; Sauer, J.; et al. Techno-economic assessment and Carbon footprint of processes for the large-scale production of Oxymethylene Dimethyl Ethers from Carbon Dioxide and Hydrogen. *Sustain. Energy Fuels* **2021**, *6*, 528–549. [[CrossRef](#)]
- Burger, J. A Novel Process for the Production of Diesel Fuel Additives by Hierarchical Design. Ph.D. Thesis, Technical University of Kaiserslautern, Kaiserslautern, Germany, 2012.
- Boyd, R. Some Physical Properties of Polyoxymethylene Dimethyl Ethers. *J. Polym. Sci.* **1961**, *50*, 133–141. [[CrossRef](#)]
- Schmitz, N.; Burger, J.; Hasse, H. Reaction Kinetics of the Formation of Poly(oxyethylene) Dimethyl Ethers from Formaldehyde and Methanol in Aqueous Solutions. *Ind. Eng. Chem. Res.* **2015**, *54*, 12553–12560. [[CrossRef](#)]
- Burger, J.; Ströfer, E.; Hasse, H. Chemical Equilibrium and Reaction Kinetics of the Heterogeneously Catalyzed Formation of Poly(oxyethylene) Dimethyl Ethers from Methylal and Trioxane. *Ind. Eng. Chem. Res.* **2012**, *51*, 12751–12761. [[CrossRef](#)]

15. Burger, J.; Ströfer, E.; Hasse, H. Production process for diesel fuel components poly(oxymethylene) dimethyl ethers from methane-based products by hierarchical optimization with varying model depth. *Chem. Eng. Res. Des.* **2013**, *91*, 2648–2662. [[CrossRef](#)]
16. Mahbub, N.; Oyedun, A.O.; Kumar, A.; Oestreich, D.; Arnold, U.; Sauer, J. A life cycle assessment of oxymethylene ether synthesis from biomass-derived syngas as a diesel additive. *J. Clean. Prod.* **2017**, *165*, 1249–1262. [[CrossRef](#)]
17. Deutz, S.; Bongartz, D.; Heuser, B.; Kätelhön, A.; Schulze Langenhorst, L.; Omari, A.; Walters, M.; Klankermayer, J.; Leitner, W.; Mitsos, A.; et al. Cleaner production of cleaner fuels: Wind-to-wheel - environmental assessment of CO₂-based oxymethylene ether as a drop-in fuel. *Energy Environ. Sci.* **2018**, *11*, 331–343. [[CrossRef](#)]
18. Artz, J.; Müller, T.E.; Thenert, K.; Kleinekorte, J.; Meys, R.; Sternberg, A.; Bardow, A.; Leitner, W. Sustainable Conversion of Carbon Dioxide: An Integrated Review of Catalysis and Life Cycle Assessment. *Chem. Rev.* **2017**, *118*, 434–504. [[CrossRef](#)]
19. Sternberg, A.; Bardow, A. Power-to-What?—Environmental assessment of energy storage systems. *Energy Environ. Sci.* **2015**, *8*, 389–400. [[CrossRef](#)]
20. Schmitz, N.; Ströfer, E.; Burger, J.; Hasse, H. Conceptual Design of a Novel Process for the Production of Poly(oxymethylene) Dimethyl Ethers from Formaldehyde and Methanol. *Ind. Eng. Chem. Res.* **2017**, *56*, 11519–11530. [[CrossRef](#)]
21. Xue, Z.; Shang, H.; Xiong, C.; Lu, C.; An, G.; Zhang, Z.; Cui, C.; Xu, M. Synthesis of polyoxymethylene dimethyl ethers catalyzed by sulfonic acid-functionalized mesoporous SBA-15. *RSC Adv.* **2017**, *7*, 20300–20308. [[CrossRef](#)]
22. Wu, J.; Zhu, H.; Wu, Z.; Qin, Z.; Yan, L.; Du, B.; Fan, W.; Wang, J. High Si/Al ratio HZSM-5 zeolite: An efficient catalyst for the synthesis of polyoxymethylene dimethyl ethers from dimethoxymethane and trioxymethylene. *Green Chem.* **2015**, *17*, 2353–2357. [[CrossRef](#)]
23. Held, M.; Tönges, Y.; Pélerin, D.; Härtl, M.; Wachtmeister, G.; Burger, J. On the energetic efficiency of producing polyoxymethylene dimethyl ethers from CO₂ using electrical energy. *Energy Environ. Sci.* **2019**, *12*, 1019–1034. [[CrossRef](#)]
24. Schmitz, N.; Burger, J.; Ströfer, E.; Hasse, H. From methanol to the oxygenated diesel fuel poly(oxymethylene) dimethyl ether: An assessment of the production costs. *Fuel* **2016**, *185*, 67–72. [[CrossRef](#)]
25. Burger, J.; Hasse, H. Processes for the production of OME fuels. In Proceedings of the Internationaler Motorenkongress, Baden-Baden, Germany, 29 August 2020. [[CrossRef](#)]
26. Ouda, M.; Mantei, F.; Hesterwerth, K.; Bargiacchi, E.; Klein, H.; White, R.J. A hybrid description and evaluation of oxymethylene dimethyl ethers synthesis based on the endothermic dehydrogenation of methanol. *React. Chem. Eng.* **2018**, *3*, 676–695. [[CrossRef](#)]
27. Oyedun, A.O.; Kumar, A.; Oestreich, D.; Arnold, U.; Sauer, J. The development of the production cost of oxymethylene ethers as diesel additives from biomass. *Biofuels Bioprod. Biorefining* **2018**, *12*, 694–710. [[CrossRef](#)]
28. Schemme, S.; Breuer, J.L.; Köller, M.; Meschede, S.; Walman, F.; Samsun, R.C.; Peters, R.; Stolten, D. H₂-based synthetic fuels: A techno-economic comparison of alcohol, ether and hydrocarbon production. *Int. J. Hydrog. Energy* **2020**, *45*, 5395–5414. [[CrossRef](#)]
29. Tönges, Y. Advances in the Production of Poly(oxymethylene) Dimethyl Ethers and Methanolic Formaldehyde Solution. Ph.D. Thesis, Technical University of Munich, Munich, Germany, 2022.
30. Towler, G.; Sinnott, R.K. *Chemical Engineering Design: Principles, Practice and Economics of Plant and Process Design*; Elsevier: Amsterdam, The Netherlands, 2012.
31. Peters, M.S.; Timmerhaus, K.D.; West, R.E. *Plant Design and Economics for Chemical Engineers*, 5th ed.; McGraw-Hill: New York, NY, USA, 2003; Volume 369, pp. 1–1006.
32. Reuss, G.; Disteldorf, W.; Gamer, A.O.; Hilt, A. Formaldehyde. In *Ullmann's Encyclopedia of Industrial Chemistry*; Wiley-VCH Verlag GmbH & Co. KGaA: Weinheim, Germany, 2000.
33. Eek Vancells, L. Method for Producing Stabilized Solutions of Formaldehyde with Methanol. U.S. Patent EP0434783B1, 17 August 1994.
34. Schmitz, N.; Breitzkreuz, C.F.; Ströfer, E.; Burger, J.; Hasse, H. Separation of water from mixtures containing formaldehyde, water, methanol, methylal, and poly(oxymethylene) dimethyl ethers by pervaporation. *J. Membr. Sci.* **2018**, *564*, 806–812. [[CrossRef](#)]
35. Dams, A.; Fried, A.; Hammann, F. Verfahren zur Gewinnung konzentrierter wäßriger Formaldehydlösungen durch Pervaporation. U.S. Patent DE4337231A1, 25 August 1993.
36. Morishita, H.; Masamoto, J.; Hata, T. Process for Producing High Purity Formaldehyde. U.S. Patent 4,962,235A, 9 October 1990.
37. Klopper, D.L.; Stevenson, L.G. Method for Making Alcoholformaldehyde Product. U.S. Patent 3,214,891A, 2 November 1965.
38. Masamoto, J.; Ohtake, J.; Kawamura, M. Process for Producing Formaldehyde and Derivatives Thereof. U.S. Patent 4,967,014, 30 October 1989.
39. Millar, G.J.; Collins, M. Industrial Production of Formaldehyde Using Polycrystalline Silver Catalyst. *Ind. Eng. Chem. Res.* **2017**, *56*, 9247–9265. [[CrossRef](#)]
40. Walker, J.F. *Formaldehyde*; Reinhold Publishing Corporation: Washington, DC, USA, 1964; pp. 2–408.
41. Ott, M. Reaktionskinetik und Destillation formaldehydhaltiger Mischungen (Berichte aus der Verfahrenstechnik). Ph.D. Thesis, Technical University of Kaiserslautern, Kaiserslautern, Germany, 2004.
42. Mann, H.J.; Pohl, W.; Simon, K.; Weigert, W. Production of free flowing paraformaldehyde. U.S. Patent 3,595,926A, 27 July 1971.
43. Ströfer, E.; Gruetzner, T.; Hasse, H.; Lang, N.; Ott, M. Verfahren zur Erzeugung Hochkonzentrierter formaldehydlösungen. U.S. Patent WO2004078678A3, 16 September 2004.
44. Ströfer, E.; Sohn, M.; Hasse, H.; Schilling, K. Highly Concentrated Formaldehyde Solution, Production and Reaction Thereof. U.S. Patent 7,193,115B2, 20 March 2007.

45. Ferre, A.; Voggenreiter, J.; Tönges, Y.; Burger, J. Demonstrationsanlage für die Synthese von OME-Kraftstoffen. *MTZ—Mot. Z.* **2021**, *82*, 28–33. [[CrossRef](#)]
46. Kuhnert, C.; Albert, M.; Breyer, S.; Hahnenstein, I.; Hasse, H.; Maurer, G. Phase Equilibrium in Formaldehyde Containing Multicomponent Mixtures: Experimental Results for Fluid Phase Equilibria of (Formaldehyde + (Water or Methanol) + Methylal) and (Formaldehyde + Water + Methanol + Methylal) and Comparison with Predictions. *Ind. Eng. Chem. Res.* **2006**, *45*, 5155–5164. [[CrossRef](#)]
47. Ott, M.; Fischer, H.H.; Maiwald, M.; Albert, K.; Hasse, H. Kinetics of oligomerization reactions in formaldehyde solutions: NMR experiments up to 373K and thermodynamically consistent model. *Chem. Eng. Process. Process. Intensif.* **2005**, *44*, 653–660. [[CrossRef](#)]
48. Brigham University. *Thermophysical Properties Laboratory Project 801*; Department of Chemical Engineering, Brigham University: Pravo, UT, USA, 2009.
49. Schmitz, N. Production of Poly(oxymethylene) Dimethyl Ethers from Formaldehyde and Methanol. Ph.D. Thesis, Technical University of Kaiserslautern, Kaiserslautern, Germany, 2018.
50. Smith, R. *Chemical Process Design and Integration*; John Wiley & Sons, Ltd.: Hoboken, NJ, USA, 2005; p. 712.
51. Christensen, P.; Dysert, L.R. Cost Estimate Classification system-as applied in engineering, procurement, and construction for the process industries—TCM Framework: 7.3—Cost Estimating and Budgeting. In *AACE International Recommended Practice No. 18R-97*; AACE: Morgantown, WV, USA, 2005; pp. 1–9.
52. Schemme, S.; Meschede, S.; Köller, M.; Samsun, R.C.; Peters, R.; Stolten, D. Property Data Estimation for Hemiformals, Methylene Glycols and Polyoxymethylene Dimethyl Ethers and Process Optimization in Formaldehyde Synthesis. *Energies* **2020**, *13*, 3401. [[CrossRef](#)]

Disclaimer/Publisher’s Note: The statements, opinions and data contained in all publications are solely those of the individual author(s) and contributor(s) and not of MDPI and/or the editor(s). MDPI and/or the editor(s) disclaim responsibility for any injury to people or property resulting from any ideas, methods, instructions or products referred to in the content.